Biological hydroxyapatite thin films synthesized by pulsed laser deposition

L. DUTA[a*], N. SERBAN[a], F. N. OKTAR[b,c,d], I. N. MIHAILESCU[a]
[a]National Institute for Lasers, Plasma and Radiation Physics, Lasers Department, Magurele, Romania
[b]Department of Bioengineering, Faculty of Engineering, Marmara University, Istanbul, Turkey
[c]Department of Medical Imaging Techniques, School of Health Related Professions, Marmara University, Istanbul, Turkey
[d]Nanotechnology and Biomaterials Application & Research Centre, Marmara University, Istanbul, Turkey

We report on biological hydroxyapatite (HA) thin films of human (dentine, DHA) and animal (bovine, BHA and ovine, OHA) synthesized by PLD. XRD studies evidenced monophasic HA structure of films, with crystallinity degree influenced by the biological origin. SEM investigations evidenced particulates with a mean size of ~2 μm. EDS analysis revealed the presence of Mg, Na, Cl, F and C besides the majority Ca and P. OHA thin films exhibited higher adherence to substrate as compared to DHA. Based upon performances and low cost manufacturing, these biomaterials could develop into a valuable competitor to commercial HA for implantology applications.

1. Introduction

Functionalization of implants' surface stands for the most advanced trend in biomaterials science. Hydroxyapatite, [HA, $Ca_{10}(PO_4)_6(OH)_2$], is nowadays the most used bioactive material for the development of the new generation of biomimetic implants, aiming for the ultimate level of biocompatibility: the perfect integration of a foreign structure into the human body. This choice is easy to understand, as the mineral constituent of skeletal systems consists of a non-stoichiometric low crystallized HA structure (50% in bone mass, 70% in bone volume) [1].

The main drawback of bulk HA ceramics is their poor mechanical properties (brittleness, incompatible elastic modulus, low fatigue endurance, low bending strength) [2]. This is the reason why the application of bulk HA bioceramics was confined for a long period of time to non load-bearing medical devices [3]. In early '80, a visionary solution emerged to overcome this limitation: the use of HA in the form of a thin coating material deposited onto load-bearing metallic implantologic objects, for whose fixation the cementation was the only option [4, 5]. This technological approach aimed to significantly improve the metallic implants osteoconductivity and to combine the mechanical advantages of metallic materials with the excellent bioactivity of the ceramic [2, 6, 7]. Such coatings should present remarkable mechanical properties and will be able to preserve the bulk excellent biological behavior [8, 9]. In recent years, a lot of efforts have been dedicated to achieve this goal, HA coatings being deposited by various techniques: plasma spraying [10], electrostatic spray deposition [11], radio-frequency magnetron sputtering [7, 12-14], electrophoretic deposition [15, 16],

sol-gel [17, 18], pulsed laser deposition (PLD) [2, 6, 19-21, 22], or combination of different techniques [23].

Laser processing of materials presents important advantages such as light processing, spectral purity, directionality, possibility to operate on very small areas (tens of nm). Generally, in PLD technique, a short UV pulsed laser beam is focused onto a rotating target, inside a vacuum chamber, in order to ablate its surface layers under controlled atmospheres [24]. The expulsed material is subsequently deposited onto a neighbor substrate. The morphological variety of the coatings, the stoichiometric transfer of the material from target to collector, the adherence of the deposited structures to substrate and the high rate film growth on surface areas placed perpendicular to the irradiated target can be achieved by a proper choice of deposition parameters.

The substrate temperature during biocompatible thin film deposition by PLD is typically in the range of 350–600°C, ensuring the growing of a highly crystalline and phase pure coating on implant materials [25]. Lower or higher substrate temperature could be chosen to fabricate films with different fine texture and roughness, depending on the coatings application. Post-deposition thermal treatments (in water vapors) have the role to restore the stoichiometry of the synthesized compound and to improve the crystalline structure of the coating.

Dentine HA (DHA), bovine-derived HA (BHA) and ovine-derived HA (OHA) are natural materials which are produced by calcination methods. HA materials prepared from human and animal resources are not dangerous when applying calcination treatments (850°C/4 hours) as it was demonstrated that no disease transmission agents can survive at such elevated temperatures [26, 27].

We report on the physical–chemical and mechanical properties of different human (dentine) and animal (ovine

and bovine)-derived HA PLD coatings, with the aim to develop a new generation of renewable materials to be used as biomimetic implant coatings.

2. Experimental

2.1 Powder preparation

HA powders of human (DHA) and animal (BHA, OHA) origin were obtained using a standard protocol described elsewhere [20].

2.2 PLD experiments

PLD depositions were conducted inside a stainless steel deposition chamber using a KrF* excimer laser source (Fig. 1), model *COMPexPro 205* (λ = 248 nm, $\tau_{FWHM} \leq$ 25 ns), running at a repetition rate of 10 Hz. The laser beam was incident on the target surface at 45°.
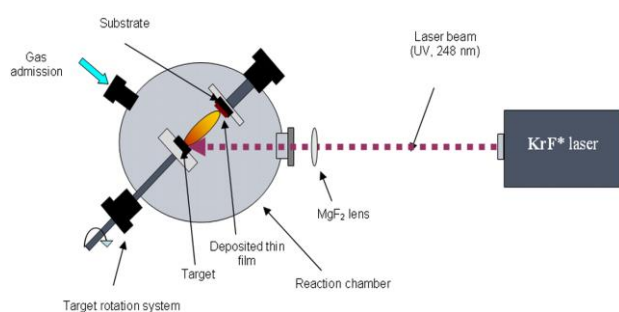

Fig. 1. PLD experimental set-up.

Two grams from each powder were pressed at 5 t in a 2 cm diameter mold, model *Specac*, and the resulting pellets were heat-treated in a furnace, model *Carbolite CF1100*, at 1100°C/4 hours to reach compactness by eliminating air bubbles and water vapors. The sintered pellets were used as targets in PLD experiments. The ablated material was collected either onto titanium (Ti) disks (1.2 cm diameter x 0.15 cm thickness), or onto Si(100) wafers (1×1) cm^2, that were placed parallel to the targets (on-axis geometry), at 5 cm separation distance in front of them. The experimental conditions were identical for both deposition substrates. Prior to introduction inside the deposition chamber, in order to eliminate the micro-impurities, the substrates were successively cleaned into an ultrasonic bath in acetone, ethanol and deionised water for 20 min and then blown dry with high purity nitrogen. The laser fluence on target was set at ~3.5 J/cm^2.

Before deposition, all HA targets were submitted to a "cleaning" process with 1000 laser pulses. During this procedure, a shutter was interposed between the target and the substrate to collect the flux of expulsed impurities. The targets were continuously rotated with 0.4 Hz and translated along two orthogonal axes in order to avoid the formation of deep craters and to insure an uniform

deposition. This also allowed exposing a "fresh" surface to the action of every laser pulse. During the experiments, the substrates were heated and maintained at a constant temperature of 500°C using a temperature controller, model *PID-EXCEL*. For the growth of one thin film, 15000 consecutive laser pulses were applied. All depositions were performed in 50 Pa water vapors. In order to restore the stoichiometry of the synthesized structures and to improve the crystalline status of the coatings, all samples were submitted to a 6 hours post-deposition thermal treatment (in water vapors), at the same temperature used during the deposition process (500°C).

2.3 Characterization of deposited structures

(*i*) X-ray diffraction (XRD) investigations were performed on a *Bruker D8 Advance* diffractometer, with Cu K$_\alpha$ (λ = 1.54 Å) radiation. The scattered intensity was scanned in the 2θ range 20–60°, with a step size of 0.04°, and 20 s/step.

(*ii*) The surface morphology of the deposited structures was investigated by Scanning electron microscopy (SEM) with a *FEI Inspect S electron* microscope. The measurements were performed in high vacuum, under secondary electrons mode. Cross-section SEM images were recorded on samples deposited on Si (100) wafers in identical conditions in order to estimate the thicknesses of the deposited structures.

(*iii*) The composition on thin films was examined by Energy dispersive X-ray spectroscopy (EDS), with a SiLi detector, model *EDAX Inc.*, operated at 20 kV.

(*iv*) The adhesion at the Ti substrate-HA films interface was measured by pull-out method, using a certified adhesion tester, model *PAT MICRO AT101*, from *DFD Instruments*, equipped with 0.28 cm diameter stainless steel test elements. They were glued onto the film's surface with a cyanoacrylate one-component epoxy adhesive, *E1100S*. The stub surface was first polished, ultrasonically degreased in acetone and ethanol and then dried in nitrogen flow. After gluing, the samples were placed in an oven for thermal curing (130°C/1hour). The pull force was smoothly increased until fracture occurred. The experimental procedure was conducted in accordance with the *ASTM D4541* and *ISO 4624* standards. Batches of 10 samples have been tested for each type of material, and a statistical estimation was performed.

3. Results and discussion

3.1 XRD

Fig. 2 displays the XRD patterns recorded in symmetrical geometry (θ-θ) for the biological HA films deposited onto Ti disks by PLD. Besides the intense peaks originating from the Ti substrate (ICDD: 44-1294), the samples consisted remarkably of a well-crystallized pure HA hexagonal phase (ICDD: 09-0432; space group P63/m). This constitutes a proof that the technological

protocol (deposition conditions and post-deposition processing) proposed in this study can accurately reproduce the HA target in terms of structure and phase purity.
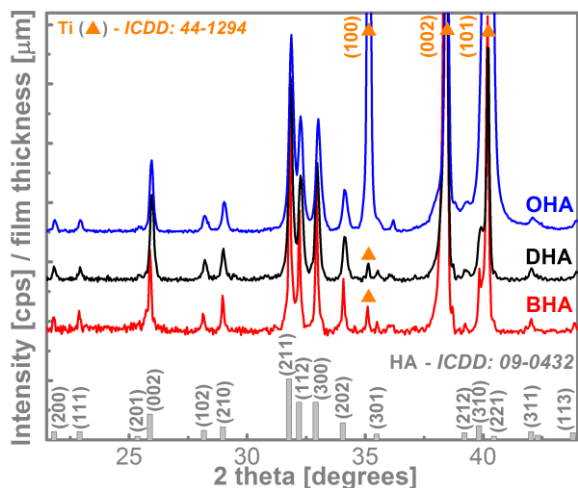

Fig. 2. XRD patterns of biological HA films.

The average crystallite size corresponding to the 002 and 300 diffraction lines of HA have been estimated using the Scherrer equation, and are collected in Table 1. The lines width was corrected for instrumental broadening using a corundum standard reference (NIST SRM 1976). A higher crystallinity, expressed by the larger crystallite size, has been evidenced for the BHA films. The growth of crystallites for the animal origin HA films (BHA and OHA) was anisotropic in shape (Table 1), whilst isotropic crystallite shape growth has been noticed for the human origin ones (DHA). At this point, we cannot assign this effect to the different origin of the materials only, because the raw material type was also different: dentine (in case of DHA) and cortical bone (in case of BHA and OHA).

Table 1. Crystallite size estimated for the 002 and 300 diffraction lines by applying the Scherrer equation.

Sample type	D_{002} [nm]	D_{300} [nm]	D_{002} / D_{300}
DHA film	55.4	52.7	~1.05
BHA film	103.8	152.8	~0.68
OHA film	71.5	53.3	~1.34

3.2 SEM-EDS

SEM micrographs (Fig. 3 a-c) revealed for the thin HA coatings a granular and rather dense morphology, mostly consisting of spherical formations structured at submicronic level: (0.8 – 3.6) μm for DHA, (1.4 – 4) μm for BHA, and (1.2 – 2.3) μm for OHA. Moreover, we noticed an agglomeration tendency in case of BHA structures (Fig. 3b), while for DHA and OHA, a rather compact layer was observed (Fig. 3-a,c). These general

morphological features are characteristic to PLD and have a favorable effect on osseointegration [27]. It has been demonstrated that rough surfaces lead to a better osseointegration as compared to smooth implants [28].

From the cross-section SEM images (Fig. 3 d-f), one can determine the following average thickness: (1.63 ± 0.15) μm for DHA, (1.29 ± 0.19) μm for BHA, and (3.3 ± 0.23) μm for OHA, with a corresponding deposition rate of (0.11 ± 0.01) nm/pulse for DHA, (0.09 ± 0.01) nm/pulse for BHA, and (0.22 ± 0.02) nm/pulse for OHA. The inferred HA films thickness can be considered suitable for osteointegrative implants' biofunctionalization, as they could ensure the implant coating sustainability in the aggressive *in vivo* environments (involving in first interaction stages the superficial film dissolution) [5]. EDS mapping of the films (data not presented here) showed a homogeneous distribution of the Ca and P cations on film surface, indicating the lack of segregation phenomena, which are usually responsible for the formation of the undesirable secondary phases. From qualitative point of view, the EDS spectra (Fig. 3 g-i) also indicated the purity of the films, so that, apart from typical bone HA constituents (Ca, P, Na, Mg, Fl, Cl, C, O), no other elemental impurities were detected. This observation is in agreement with the XRD data (Fig. 2), which pointed out to the formation of single phase apatitic films on the Ti substrates.
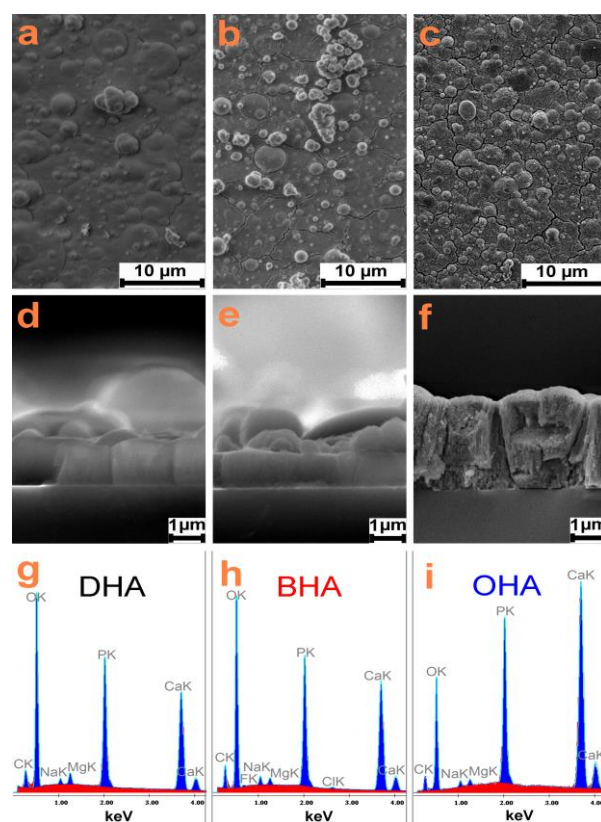

Fig. 3. Typical SEM micrographs recorded in top-view (a,b,c) and cross-view modes (d,e,f) for DHA (a,d), BHA (b,e), and OHA (c,f) films. EDS spectra collected for the DHA (g), BHA (h) and OHA (i) films.

Quantitative EDS analyses were performed on the PLD thin films in order to estimate the Ca/P atomic ratio. The calculated values are collected in Table 2, and show that a sub-stoichiometric target-to-substrate transfer occurred for HA films. Similar Ca/P atomic ratios were obtained by Duta *et al.* [20], which assumed that these values should ensure high osseoconductivity values and fast osseointegration rates of implants covered with these types of coatings.

Table 2. Ca/P atomic ratio of the PLD targets and films, as determined by EDS analysis.

	Ca/P molar ratios		
	DHA	**BHA**	**OHA**
Target	1.57 ± 0.03	1.62 ± 0.02	1.51 ± 0.02
Film	1.54 ± 0.03	1.58 ± 0.02	1.37 ± 0.03

3.3 Pull-out adherence

The test dollies were glued in the center of each sample surface. Adhesive failure occurred each time at the substrate-film interface. The bonding strength values are presented in Table 3.

Table 3. Pull-out bonding strength values of HA films.

Sample type	Pull-out adherence value [MPa]
DHA film	*50.1 ± 4.9*
BHA film	*41.9 ± 6.4*
OHA film	*68.4 ± 1.7*

Similar values of adherence have been recorded for PLD and sputtered HA films, whilst lower values have been determined for other deposition techniques (Table 4).

Table 4. Pull-out bonding strength values of HA films obtained by various deposition techniques.

Deposition technique	Pull-out adherence value [MPa]
Sol-Gel	30-40 [*Refs. 18, 29*]
Plasma-spraying	18-26 [*Refs. 30, 31*]
Magnetron sputtering	50-85 [*Refs. 7, 12, 13*]
Pulsed-Laser deposition	50-75 [*Refs. 20, 32*]
Electrophoretic deposition	21-35 [*Ref. 33*]

The adhesion strength at the coating-substrate interface is a critical parameter for successful implantation and long-term stability of implant-type structures. Currently, an adherence value higher than 51 MPa only is considered acceptable for these types of implant coatings

[8, 9]. The excellent values of adherence obtained for OHA thin films should be therefore emphasized.

4. Conclusions

We conducted a comparative study of biological hydroxyapatite (HA) films of human and animal origin. The existence of well-crystallized HA was clearly detected in all deposited films. The highest degree of crystallization was reached in case of BHA films. Morphological investigations evidenced the existence of a granular surface which is considered adequate for this type of medical applications. We observed by EDS the presence of Mg, Na, Cl, F and C oligoelements which are characteristic to healthy human bone. The highest adherence to Ti substrate, of ~69 MPa, was measured in case of OHA films.

These results support the suggestion that the coatings could allow for obtaining new implants for orthopaedic and stomatology applications, with shorter osseointegration time and better osseoconductive characteristics. We also mention that all films were obtained from renewable resources.

References

[1] C. V. M. Rodriguesa, P. Serricella, A. B. R. Linhares, R. M. Guerdes, R. Borojevic, M. A. Rossi, M. E. L. Duarte, M. Farina, Biomaterials **24**, 4987 (2003).
[2] B. Leon, J. Jansen, Thin Calcium Phosphate Coatings for Medical Implants, Springer Science + Business Media, New York (2009).
[3] S. V. Dorozhkin, Mater. Sci. Eng. C **33**, 3085 (2013).
[4] S. V. Dorozhkin, Biomaterials **31**, 1465 (2010).
[5] J. A. Epinette, M. T. Manley, R. G. T. Geesink, Fifteen Years of Clinical Experience with Hydroxyapatite Coatings in Joint Arthroplasty, first ed., Springer-Verlag, Paris (2003).
[6] L. Duta, G. E. Stan, A. C. Popescu, G. Socol, F. M. Miroiu, I. N. Mihailescu, A. Ianculescu, I. Poeata, A. Chiriac, Proc. 10-th Conf. Micro- to Nanophotonics III, Ed. V. I. Vlad, SPIE, 2013, p. 888208-1.
[7] L. E. Sima, G. E. Stan, C. O. Morosanu, A. Melinescu, A. Ianculescu, R. Melinte, J. Neamtu, S. M. Petrescu, J. Biomed. Mater. Res. A **95A**, 1203 (2010).
[8] ISO 13779 – 2 Implants for surgery – Hydroxyapatite

– Part 2: Coatings of hydroxyapatite.
http://www.iso.org/iso/iso_catalogue/catalogue_tc/catalog
ue_detail.htm?csnumber=43827 (2008).

[9] Food and Drug Administration [FDA], Calcium phosphate (Ca–P) coating draft guidance for preparation of FDA submissions for orthopedic and dental endooseous implants, 1997, p. 1.

[10] G. L. Zhao, G. Wen, Y. Song, K. Wu, Mater. Sci. Eng. C **31**, 106 (2011).

[11] S. Leeuwenburgh, J. Wolke, J. Schoonman, J. Jansen, Thin Solid Films **472**, 105 (2005).

[12] S. J. Ding, Biomaterials **24**, 4233 (2003).

[13] G. E. Stan, J. Optoelectron. Adv. M **11**, 1132 (2009).

[14] J. Neamtu, G. E. Stan, C. Morosanu, C. Ducu, A. Popescu, I. N. Mihailescu, J. Optoelectron. Adv. M **9**, 3821 (2007).

[15] M. Mihailović, A. Patarić, Z. Gulišija, D. Veljović, D. Janaćković, Chem. Ind. Chem. Eng. Q **17**, 45 (2011).

[16] A. R. Boccaccini, S. Keim, R.Ma, Y. Li, I. Zhitomirsky, J. R. Soc. Interface **7**, S581 (2010).

[17] T. F. Stoica, C. Morosanu, A. Slav, T. Stoica, P. Osiceanu, C. Anastasescu, M. Gartner, M. Zaharescu, Thin Solid Films **516**, 8112 (2008).

[18] D. M. Liu, Q. Yang, T. Troczynski, Biomaterials **23**, 691 (2002).

[19] G. Socol, A. M. Macovei, F. Miroiu, N. Stefan, L. Duta, G. Dorcioman, I. N. Mihailescu, S. M. Petrescu, G. E. Stan, D. A. Marcov, A. Chiriac, I. Poeata, Mater. Sci. Eng. B **169**, 159 (2010).

[20] L. Duta, F. N. Oktar, G. E. Stan, G. Popescu-Pelin, N. Serban, C. Luculescu, I. N. Mihailescu, Appl. Surf. Sci. **265**, 41 (2013).

[21] L. Duta, G. Socol, F. Sima, I. N. Mihailescu, G. E. Stan, D. A. Marcov, L. E. Sima, S. M. Petrescu, A. Melinescu, A. Ianculescu, A. Chiriac, I. Poeata, Proc. 2-nd Advanced Technologies for Enhanced Quality of Life, ATEQUAL, 2010, p. 127.

[22] M. Jelínek, T. Kocourek, K. Jurek, J. Remsa, J. Mikšovský, M. Weiserová, J. Strnad, T. Luxbacher, Appl. Phys. A **101**, 615 (2010).

[23] M. Roy, V. K. Balla, A. Bandyopadhyay, S. Bose, Acta Biomater. **7**, 866 (2011).

[24] R. Eason, Pulsed Laser Deposition of thin films – Applications-led growth of functional materials, Wiley-Interscience (2007).

[25] K. K. Saju, R. Reshmi, N. H. Jayadas, J. James, M. K. Jayaraj, Proc. Inst. Mech. Eng. Part H J. Eng. Med. **223**, 1049 (2009).

[26] G. Goller, F. N. Oktar, S. Agathopoulos, D. U. Tulyaganov, J. M. F. Ferreira, E. S. Kayali, I. Peker, J. Sol-Gel Sci. Techn. **37**, 111 (2006).

[27] L. S. Ozyegin, F. N. Oktar, G. Goller, S. Kayali, T. Yazici, Mater. Lett. **58**, 2605 (2004).

[28] D. M. Brunette, P. Tengvall, M. Textor, P. Thomsen, Titanium in Medicine, Springer, Berlin (2001).

[29] N. Hijón, M. Victoria Cabañas, J. Peña, M. Vallet-Regí, Acta Biomater. **2**, 567 (2006).

[30] C.-C. Chen, T.-H. Huang, C.-T. Kao, S.-J. Ding, J. Biomed. Mater. Res. B **78B**, 146 (2006).

[31] Y. Duan, S. Zhu, F. Guo, J. Zhu, M. Li, J. Ma, Q. Zhu, Arch. Med. Sci. **8**, 199 (2012).

[32] F. J. Garcia-Sanz, M. B. Mayor, J. L. Arias, J. Pou, B. León, M. Perez-Amor, J. Mater. Sci-Mater. M **8**, 861 (1997).

[33] C. Lin, H. Han, F. Zhang, J. Mater. Sci-Mater. M **19**, 2569 (2008).

[*]Corresponding author: liviu.duta@inflpr.ro